Sci. Bull. Fac. Educ., Nagasaki Univ., No.32, pp. 21~36 (1981)

# Vapor Growth of $SnO_2$ Single Crystals From $SnI_4$ and their Growth Mechanisms

Masami HIROSE and Yoshio FURUYA*

Faculty of Education, Nagasaki University, Nagasaki 852

*National Defense Academy, Yokosuka 239

(Received Oct. 31 1980)

**Abstract**

Vapor growth of $SnO_2$ single crystals, belonging to rutile-type crystals, has tried by the reaction of $SnI_4$ vapor with $O_2$ gas or $H_2O$ vapor. $SnO_2$ single crystals more easily crystallized by hydrolysis than by oxidation of $SnI_4$, and the optimum temperature range of the growth region was between 1200 ℃ and 1250 ℃ in the oxidation and between 1100 ℃ and 1150 ℃ in the hydrolysis, respectively. From the detail observations of the characteristic crystals grown by the hydrolysis, it was made clear that the leaf-type elongated by the growth of <110> needles and thickened by the deposition and diffusion on the surfaces succeeded to the elongating growth, that the pyramid-type elongated and thickened by the two dimensional layer growth and that the plate-type thickened by the two dimensional layer growth. The leaf and pyramid-types tended to crystallize to an octahedron consisting of the {101} and {011} facets though their growth mechanisms were different.

## 1. Introduction

Vapor growth of $SnO_2$ single crystals, belonging to rutile-type crystals, has been attempted from some starting materials to examine the intrinsic electrical and optical properties, and the growth conditions and crystalline habits have been reported [1—4]. In these reports, high growth temperatures and long runnings for the growth of $SnO_2$ single crystals have been required.

Previously, present authors and one of the authors have tried the vapor growth of ZnO single crystals, belonging to wrutzite-type crystals, by oxidation and hydrolysis of $ZnI_2$, one of zinc halides, and reported the growth conditions, crystalline habits and crystallographic perfections, and discussed the growth mechanisms of needle and plate, which were typical crystalline habits of the grown ZnO single crystals, by being based on the characteristic features of the obatined crystals [5—7]. In those growth experiments, where the starting material, $ZnI_2$, and the

reaction material, $O_2$ or $H_2O$, were transported continuously to the growth region, it had been expected that the grown ZnO single crystals had growth markings suggesting each stage of the growth by the reason that the growth was stopped in a state out of equilibrium.

Concerning the vapor growth of $SnO_2$ single crystals from stannic halides as a starting material, M. Nagasawa et al. [8] and C. G. Fonstad et al. [9] have reported the growth by vapor reaction of $SnCl_4$ with $H_2O$. But, that from stannic iodide has not been tried and, moreover, the growth mechanisms of $SnO_2$ single crystals from the vapor phase have not been made clear yet. Therefore, the growth of $SnO_2$ single crystals by vapor reaction of $SnI_4$ with $O_2$ or $H_2O$ was carried out by modifying partially the experimental arrangement used for the growth of ZnO single crystals.

As the results, $SnO_2$ single crystals remarkably grew in the reaction of $SnI_4$ with $H_2O$, and the growth temperature was comparatively low and the growth rates were large. Moreover, many characteristic $SnO_2$ single crystals which suggested their growth mechanisms were obtained, as was expected. In present paper, the growth conditions of $SnO_2$ single crystals by the vapor reaction of $SnI_4$ and the crystalline habits and growth mechanisms of leaf, pyramid and plate-type $SnO_2$ single crystals, which are typical crystalline habits in present growth experiments, are reported.

## 2. Growth procedure

Schema of the experimental arrangement used for the growth of $SnO_2$ single

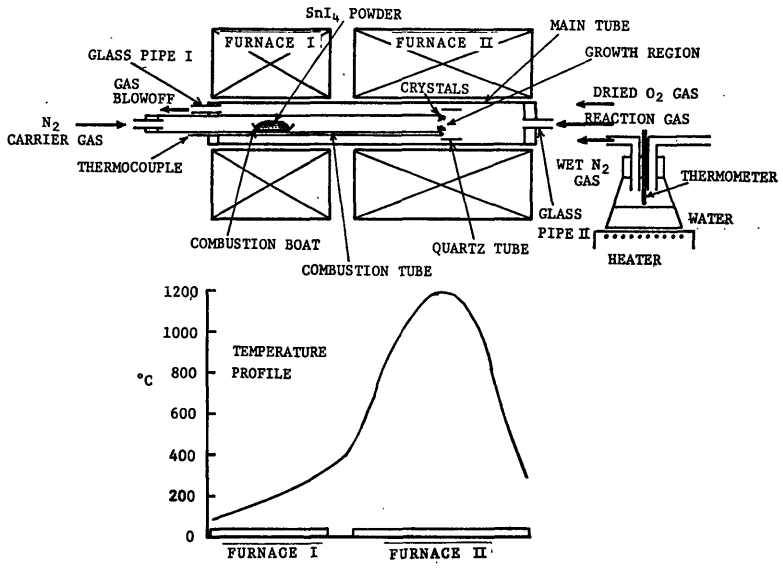


Fig. 1. Schema of the experimental arrangement used for the growth of $SnO_2$ single crystals and an example of its temperature profile.

crystals and an example of its temperature profile are shown in Fig. 1. The arrangement is made up of two electric furnaces, I and II, a horizontal alumina muffle tube (50 mm in internal diameter and 1000 mm in length), which is main tube, through the furnaces, a combustion tube (20 mm in internal diameter) fixed horizontally in the main tube, a quartz tube (35 mm in internal diameter and 60 mm in length) located at the central part of the furnace II to disturb the rapid diffustion of reacting materials and two glass pipes, one for inflow of reaction gases and another for exhaust. About 30 grams of $SnI_4$ powder (99.9% in purity) as the starting material was charged in a combustion boat and placed at the central part of the furnace I inside the combustion tube. As a material reacted with $SnI_4$, dried $O_2$ gas or $H_2O$ vapor was prepared as the case of the growth experiments of ZnO single crystals from $ZnI_2$. The main tube was filled by $N_2$ gas until the temperatures of the furnaces attained at the appointed ones. The $SnI_4$ powder was heated at a temperature between 190 ℃ and 200 ℃ which was beyond its sublimation temperature and the $SnI_4$ vapor sublimated was transported through the combustion tube to the growth region, which was the central part of the furnace II in the main tube, by dried $N_2$ gas which was used as a carrier gas. On the other hand, the dried $O_2$ gas or $H_2O$ vapor was carried into the growth region through the glass pipe II to be made a reacting atmosphere. Dried $N_2$ gas was also used as a carrier gas for the transportation of $H_2O$ vapor, and two kinds of wet $N_2$ gas, which were higher saturated wet $N_2$ gas and lower one, were produced while the dried $N_2$ gas passed through a glass flask filled with half full of water which was maintained at the temperature of 100 ℃ or at room temperature. The temperature of the growth region was varied between 1000 ℃ and 1300 ℃ by each growth running in order to determine the optimum growth temperature in either case of the growth reactions of $SnI_4$ vapor with dried $O_2$ gas and wet $N_2$ gas. The flow rates of dried $N_2$ carrier gas ot $SnI_4$ vapor and dried $O_2$ or wet $N_2$ reaction gas were maintained about 230 cc/min and 150 cc/min in every growth runnings, respectively.

After growth runnings of several hours, many crystals and powder were observed around the tip of combustion tube. These grown crystals and powder were identified as $SnO_2$ crystals and $SnO_2$ powder by X-ray diffraction method, respectively, and each crystal was certified to be a single crystal by the Divergent X-ray method [11].

### 3. Growth conditions and morphologies

When the dried $O_2$ gas was prepared as a reaction gas, the growth of $SnO_2$ single crystals was not noticeable, and the typical close-up, as grown after a 5 hours running, is shown in Fig. 2(a). The grown $SnO_2$ single crystals were small and dendritic and a great deal of powdery $SnO_2$ was always attended. The color of these crystals and powder were white. The optimum range of the temperature of growth region was between 1200 ℃ and 1250 ℃. Large $SnO_2$ single crystals grew

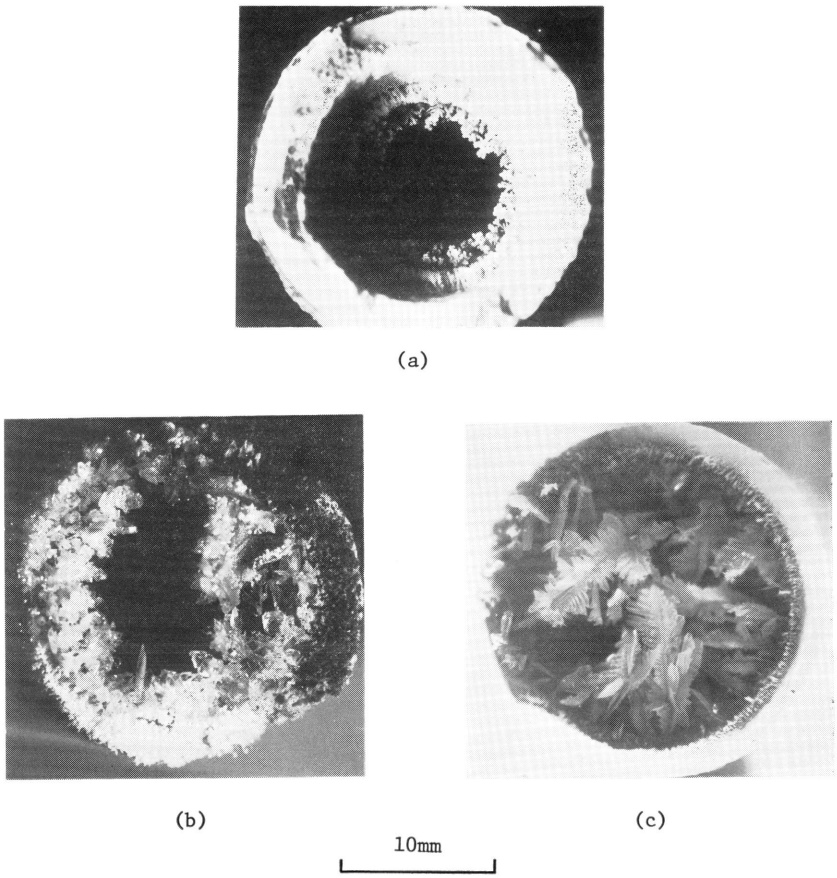


Fig. 2. Close-ups, as grown, of $SnO_2$ single crystals growing around the tip of the combustion tube. (a) By the reaction of $SnI_4$ with $O_2$ gas, (b) by the reaction with higher saturated wet $N_2$ gas and (c) by the reacton with lower saturated wet $N_2$ gas.

when the wet $N_2$ gas was prepared as a reaction gas and when the temperature of growth region was maintained at a temperature between 1100 ℃ and 1150 ℃. Figures 2(b) and 2(c) show the close-ups, as grown after a 5 hours running, of $SnO_2$ single crystals grown by the reaction of $SnI_4$ with $H_2O$ ; (b) is in the case of higher saturated wet $N_2$ gas and (c) lower saturated one. The growth of $SnO_2$ single crystals is more remarkable in the reaction with lower saturated wet $N_2$ gas than with higher saturated one. Powdery $SnO_2$ was not obtained at all in the both reactions of $SnI_4$ with $H_2O$. In order to examine the influence of the diffusion of reaction materials from the outside air through the interstices etc. of the arrangement on the growth of $SnO_2$ crystals and the production of powdery $SnO_2$, which has been pointed out by B. Thiel et al. [4], some growth runnings were performed under

the growth condition only without preparing the reaction gas. As the results, no $SnO_2$ crystals and powdery $SnO_2$ were observed.

From these experimental facts, it is made clear that when the growth temperature is maintained at a temperature between 1200 ℃ and 1250 ℃, the growth of $SnO_2$ single crystals and the production of powdery $SnO_2$ are advanced by the oxidation expressed by next chemical equation:

$$SnI_4 + O_2 = SnO_2 + 2I_2,$$

and when it is maintained at a temperature between 1100 ℃ and 1150 ℃, the growth of $SnO_2$ single crystals by the hydrolysis of $SnI_4$ :

$$SnI_4 + 2H_2O = SnO_2 + 4HI.$$

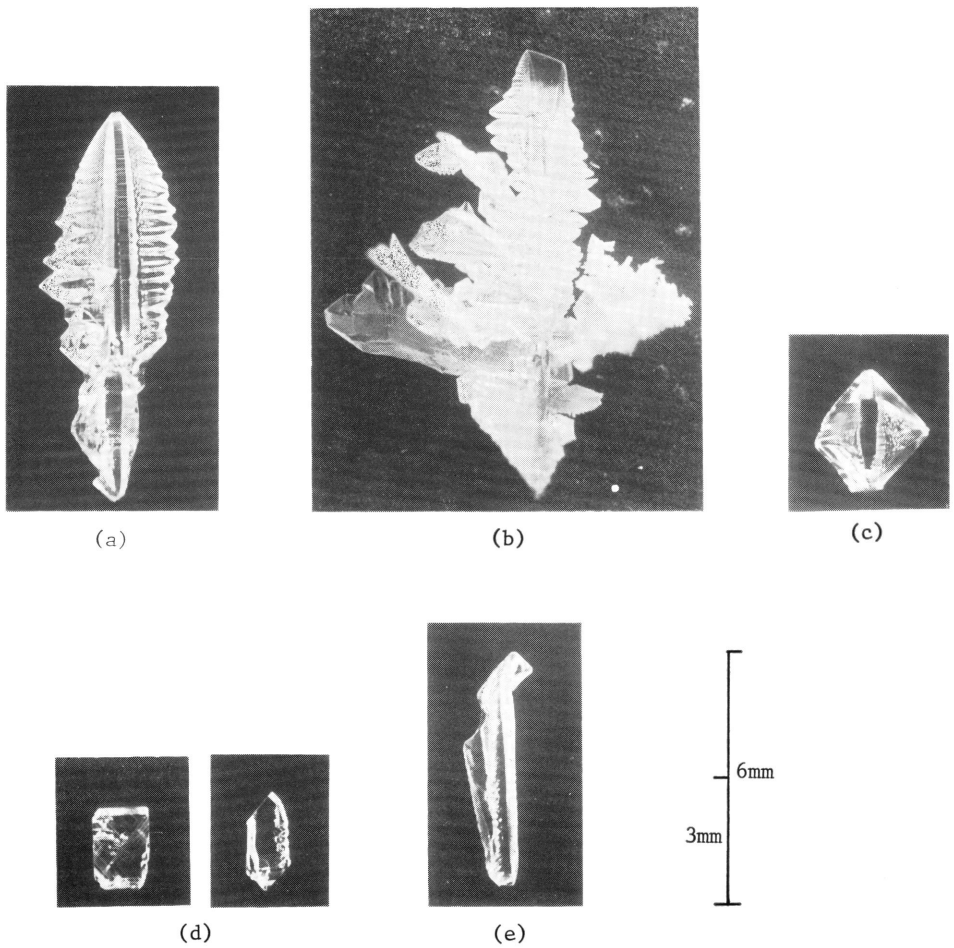


Fig. 3. Close-ups of various type $SnO_2$ single crystals grown by the hydrolysis. Each crystal is designated as follows for convenience sake : (a) leaf-type, (b) dendrite-type, (c) pyramid-type, (d) plate-type and (e) hollow-type, respectively.

Moreover, from the comparison of the growing states shown in Figs. 2(a), (b) and (c), it is recognized that the crystallization of $SnO_2$ single crystals easily advanced by the hydrolysis of $SnI_4$ than by the oxidation of $SnI_4$, and that it is more easily advanced by the reaction of $SnI_4$ with lower saturated wet $N_2$ gas than with higher saturated one.

Various types of $SnO_2$ single crystals obtained after each running of 5 hours by the hydrolysis of $SnI_4$ are shown in Fig. 3. We have designated (a), (b), (c), (d) and (e) as leaf, dendrite, pyramid, plate and hollow-type $SnO_2$ single crystals from their morphologies as a matter of convenience, respectively. They were colorless and transparent or semi-transparent for their incomplete surfaces. A characteristic region is observed at the center of the leaf and pyramid-types along their lengthwise directions as if it was a trace of growth axis. The dendrite-type, which were consisted of many leaf-type single crystals, grew mainly in the reaction with lower saturated wet $N_2$ gas and the pyramid and plate-type single crystals grew mainly in the reaction with higher saturated wet $N_2$ gas, and in the plate-type two kinds were distinguished as is shown in Fig. 3(d). The growth of the leaf and hollow-type single crystals were found in the both reactions of hydrolysis. The hollow-type had a groove or a hollow due to three or four enclosed surfaces in the lengthwise direction. The grown $SnO_2$ single crystals are generally larger in the reaction with lower saturated wet $N_2$ gas, though they are more frail, than with higher saturated one.

## 4. Crystallographic properties

### 4—1. Crystalline habits

The crystalline habits of the leaf, pyramid and plate-type $SnO_2$ single crystals were investigated by a gonio-microscope. In this investigation, the orientations of crystal axes and the indices of crystal faces were determind by comparing observed facial angles with those theoretically calculated. And, the lattice parameters determined by W. H. Baur [10], which were supported by another investigator [8] and fairly coincided with ones given by T. Takizawa et al. [3], i.e. $a=b=4.737$ Å, $c=3.185$ Å, were used in the theoretical calculation.

The crystalline habits of the leaf and pyramid-type $SnO_2$ single crystals are shown in Figs. 4(a) and (b), schematically. Though the leaf-type $SnO_2$ single crystal has complicated surfaces as a whole and imperfect parts are observed on their surfaces, many a little-developed {101} and {011} faces which make up gables-like structures are found at the edges. The pyramid-type $SnO_2$ single crystal has eight well-developed {101} and {011} faces building up an octahedron. In the both-types, the characteristic regions parallel to [110] direction are sketched at the central part of them, as is found in Figs. 3(a) and (c). Figure 4(c) shows a scanning electron microphotograph of the part of the characteristic region and the gables-like structure of the leaf-type $SnO_2$ single crystal. From this figure, it is

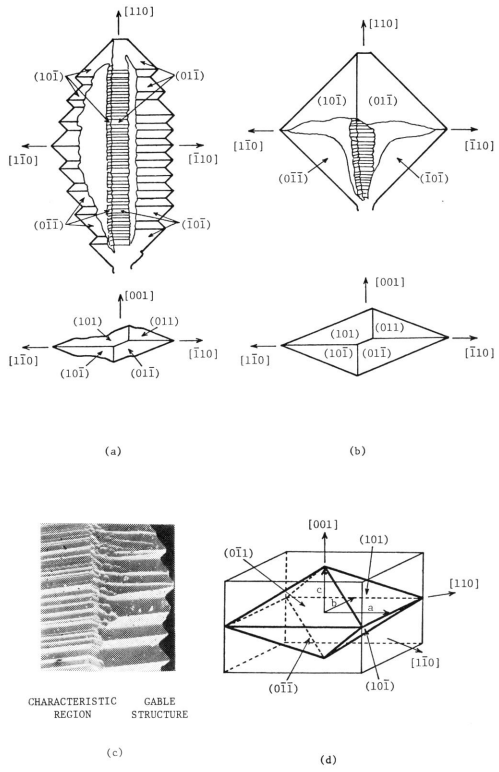


Fig. 4 Crystalline habits of the leaf and pyramid-type $SnO_2$ single crystals. (a) The leaf-type and (b) the pyramid-type. (c) A scanning electron microphotograph of a part of the leaf-type. (d) An idealized sketch of an octahedron consisted of {101} and {011} facets.

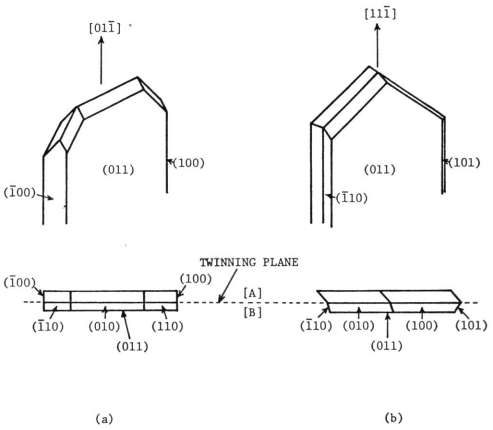


Fig. 5. Crystalline habits of the plate-type $SnO_2$ single crystals. (a) The <011> plate and (b) the <111> plate.

found that the characteristic region is a gathering of small gables which is also made up by numerous slightly developed {101} and {011} faces. The growth axes of both-type $SnO_2$ single crystals are [110] directin. An idealized sketch of their crystallization property guessed from these investigations is shown in Fig. 4(d). as to help the understanding for their crystallographic property.

The plate-type $SnO_2$ single crystals have well-developed {011} faces. Two kinds of the plates may be distinguished by their crystal axes. Their crystalline habits are schematically shown in Fig. 5. Figues 5(a) and (b) are named as <011> plate and <111> plate, respectively. The lateral surfaces are made up by {100} and {110} faces in the <011> plate and by {100}, {110} and {101} faces in the <111> plate. The {011} twinning plane which is pointed out by M. Nagasawa et al. [8] is clearly recognized in the both kinds of plates, that is, [A] and [B] denoted in Fig. 5 are the relation of twin, one another. The {011} twinning planes are also recognized in the hollow-type $SnO_2$ single crystals, but they are not uncertain in the leaf and pyramid-types. Although the hollow-types have complicated external

structures due to the twinning planes and are interesting crystallographically, they are not explained in present paper.

4 — 2. Internal structures

The internal structures of the leaf and <011> plate-type $SnO_2$ single crystals were observed by the Divergent X-ray method [11], in which the distance from the X-ray micro-focus on the anode to the specimen was 100 mm and the one from the specimen to the film was 32 mm. The specimen clamped vertically by cement on a goniometer was struck by the divergent white X-rays which were emitted from a

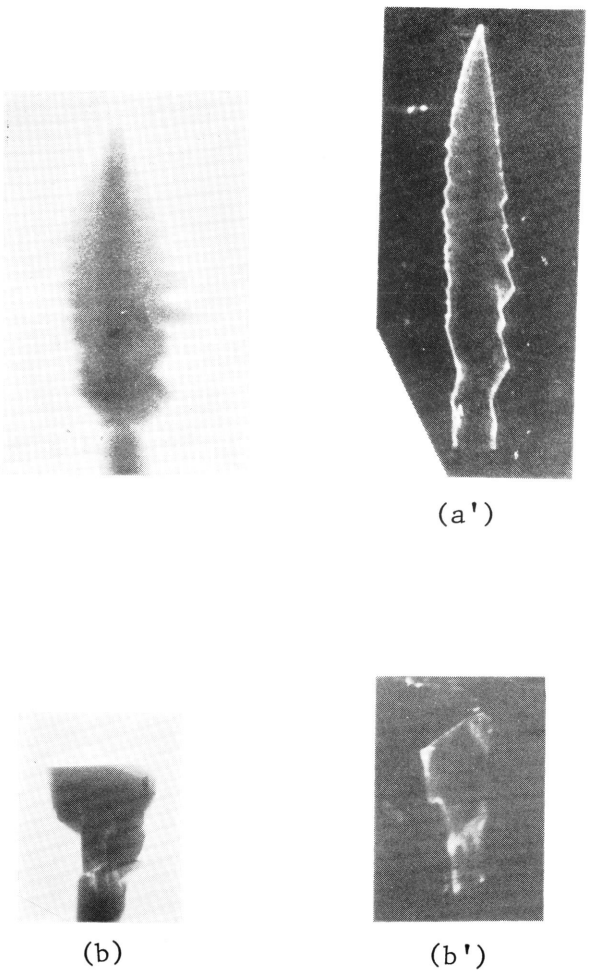


Fig. 6. Divergent X-ray radiographs of the leaf and <011> plate-type $SnO_2$ single crystals. (a) and (a') show the image of the central black part and a broad Laue-spot of the leaf-type, respectively. (b) and (b') show ones of the <011> plate-type, respectively.

micro-focus on Ag anode, whose apparent size was about 0.05 x 0.05 $mm^2$. The applied voltage and beam current were 46 kV and 0.2 mA, respectively. The duration of the exposure for taking the Laue-spots and that of the central black part were about 35 hours and 30 seconds respectively, and the Fuji Softex F. G. films were used. The axis of the incident Divergent white X-ray is parallel to [001] direction of the leaf and perpendicular to (011) surface of the <011> plate. Figures 6 (a) and (a′) show the image of central black part and a broad Laue-spo t in the Divergent X-ray radiograph of the leaf-type respectively. Similarly, Fig. 6(b) and (b′) show those of the <011> plate-type. These figures indicate that their internal structures and their singlarities are fairly good, though a traceable pattern in the [110] lengthwise direction, which correspond to the characteristic region, is observed in the radiographs of the leaf-type $SnO_2$ single crystals.

## 5. Growth mechanisms

Mean growth rates of the leaf, pyramid and plate-type $Sno_2$ single crystls, which were estimated from the averaged sizes of each type and the time of each growth running, are shown in Fig. 7 for some principal directions. The values of the leaf-type are larger than ones of the other-types in <110> direction. Especially, in the growth of [110] direction, the leaf-type is three times or more as large as the pyramid-type in spite of the same crystallization property. This will suggest that the growth mechanism of the leaf-type differs from the other-types. In the <011> and <111> plate-types, their mean growth rates along the crystal axes are almost equal, and ones of the pyramid-type are the smallest of all types.

| DIRECTIONS / TYPES | [110] | [$\bar{1}$10] | [001] | [01$\bar{1}$] | [11$\bar{1}$] |
|---|---|---|---|---|---|
| LEAF | 23.8 | 11.9 | 3.2 | – | – |
| PYRAMID | 6.7 | 6.7 | 2.0 | – | – |
| <011> PLATE | – | – | – | 8.3 | – |
| <111> PLATE | – | – | – | – | 8.5 |

( in μm/min )

Fig. 7. Mean growth rates in principal directions of leaf, pyramid and plate-type $SnO_2$ single crystals.

### 5 – 1. Leaf-type

Close-ups of dendritic crystals, which were obtained successfully in shortened runnings of the growth experiments, are shown in Figs. 8 (a) and (b). They were in contact with the inside wall of the combustion tube at the point of markings ↑ in this figures, which was the starting point of the growth. The dendritic crystal shown in Fig. 8 (a) offers a <110> needle structure which consists of a [110] needle and [$\bar{1}$10] needles growing from the one side of the [110] needle. Figure 8 (b) shows a further advanced stage of the growth of the dendritic crystal showing in Fig. 8 (a). In this stage, the thickening growth of the [110] needle and the [$\bar{1}$10] needles are observed in addition to their elongating growth and the spaces between the [$\bar{1}$10] needles are filled. Moreover, it is found that the [1$\bar{1}$0] needles

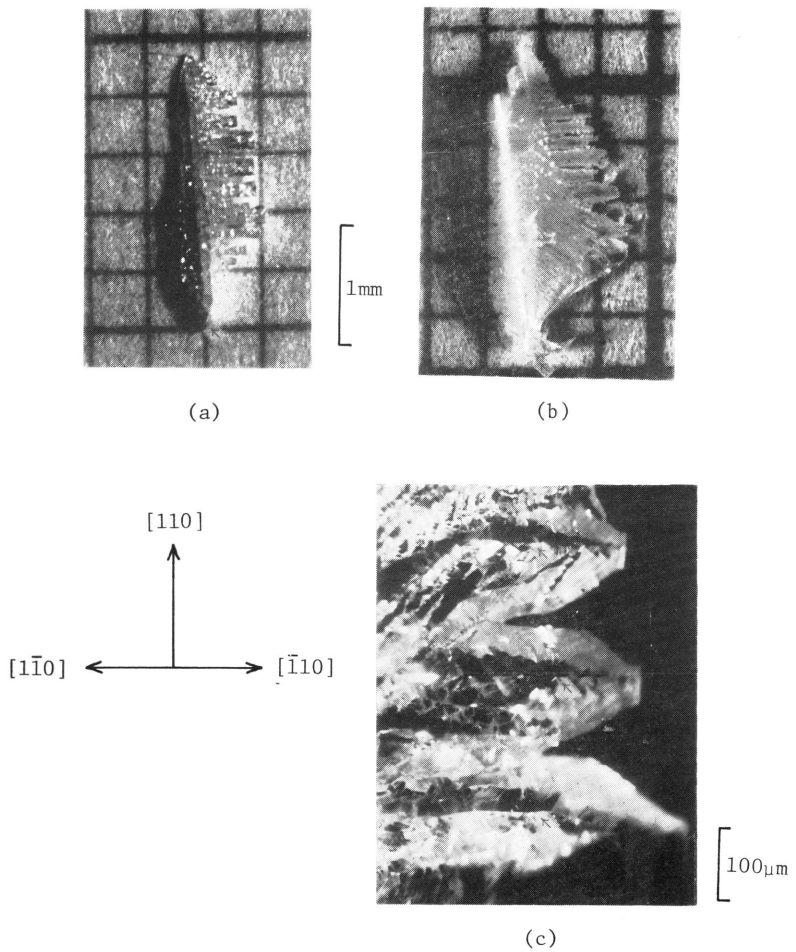


Fig. 8. Dendritic crystals suggesting the growth mechanism of a leaf-type $SnO_2$ single crystal. (a) A close-up of the dendritic crystal obtained in earlier stage of the growth. (b) One in the further advanced stage of the growth. (c) An optical microphotograph of the <110> second needles being in the midst of the thickening growth.

which are crystallographically equal to the [$\bar{1}$10] needles grow from the another side of the [110] needle, though they are small. The [110] needle and the [$\bar{1}$10] and [1$\bar{1}$0] needles growing from both sides of the [110] needle are called, respectively, as a first needle and second needles for convenience sake. The deviation of growth between the second needles, [$\bar{1}$10] ans [1$\bar{1}$0], will be originated by the unequal preparation of $SnO_2$ molecules around the first needle. The development of faces is hardly observed yet in these stages. Figure 8(c) shows an optical microphotograph of the second needles being in the midst of the thickening growth. The edge-lines of each gable, denoting by markings ↑, are slightly observed at the

center along the lengthwise direction of the needles.

An optical microphotograph of a leaf-type $SnO_2$ single crystal which will grow through the each stage shown in Fig. 8 are shown in Fig. 9(a). The gables-like structures, denoted by [A], and the characteristic region, by [B], which are made up of {101} and {011} faces as is mentioned in earlier section, are observed. Figure 9(b) shows a scanning electron microphtograph in left-side view of the leaf-type $SnO_2$ single crystal showing in Fig. 9(a). Pyramidal patterns denoted by markings ↑ in this figure, which are marks of the tip ends of second needles, are observed correspondingly to every gables. Therefore, it is clearly considerable that the characteristic region and the gables-like structures are corresponding to the first needle and the second needles, respectively. The {101} and {011} faces are developed from the edges and are not appeared at the central part of the crystal except the characteristic region. As this reason, it is offered that the edges are higher than the central part in supersaturation, and that the thickness in [001] direction is the largest at the center and decreases toward the edges as the result that the leaf-type tend to crystallize into an octahedron-shape consisting of eight {101} and {011} facets as is shown in Fig. 4(d) so that the surface energy of the leaf-type may become the lowest.

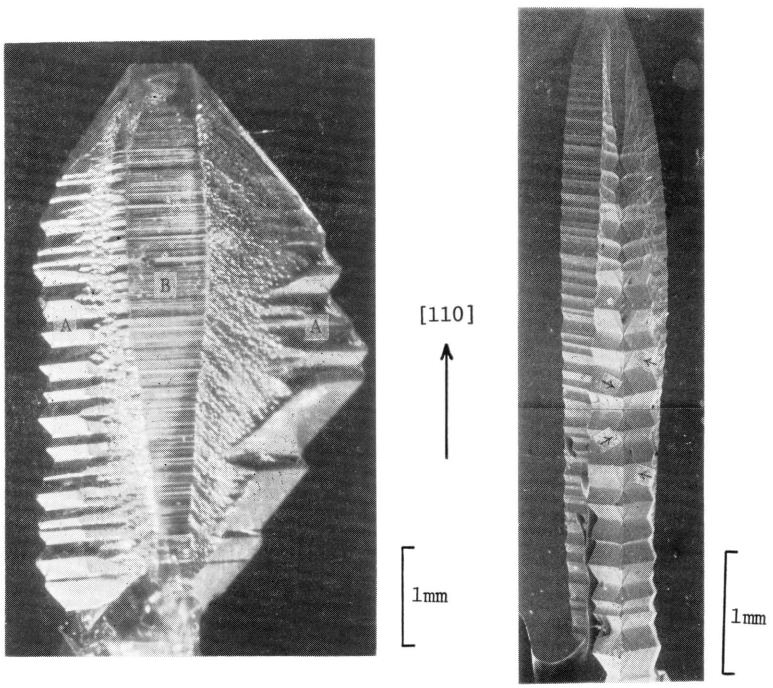


Fig. 9. A leaf-type $SnO_2$ single crystal grown through the each stage shown in fig. 8. (a) An optical microphotograph. (b) A scanning electron microphotograph of the left-side view.

From these observations of the characteristic figures as is shown in Figs. 8 and 9, it is concluded that the growth of a leaf-type is proceeded by the manner that a [110] needle grow first and $[\bar{1}10]$ and $[1\bar{1}0]$ needles do secondly from the both sides of the [110] needle, perpendicularly one after another, and then the gables-like structures corresponding to the <110> second needles and the characteristic region corresponding to the [110] first needle are formed by the deposition and diffusion of the molecules from the edges, where the supersaturation is higher, as the result of the thickening growth of each needle successive to the elongating growth in which the dendritic crystal tend to crystallize into an octahedron-shape as the final stage of the growth. That is, though the mechanism of elongating growth of these <110> needles is not clear in present experiments, two-steps: the elongating growth due to the preceding needles and the thickening growth, which are recognized in the growth of the plate-type ZnO single crystals by vapor reaction of $ZnI_2$ with $H_2O$, are also recognized in the growth of leaf-type $SnO_2$ single crystals.

5 — 2. Pyramid-type

Figure 10 shows scanning electron microphotographs of the $SnO_2$ single crystals suggesting the growth mechanism of a pyramid-type. These crystals are also obtained in shortened growth runnings by the reaction of $SnI_4$ with higher saturated wet $N_2$ gas and the markings ↑ in the figures indicate the starting point of growth. Figure 10(a) offers a rod-like $SnO_2$ single crystal having four faces, (101), $(10\bar{1})$, (011) and $(01\bar{1})$, on which some bunching steps are observed, at the top and having stepped surfaces from the central part to the root. From this characteristic figure, it can be guessed that the growth in the [110] direction, the elomgating growth, is advanced by two dimensional layer growth from the tip edge, where the supersaturation is higher, on the (101), $(10\bar{1})$, (011) and $(01\bar{1})$ faces as these four faces are always expoused at the top. Figure 10(b) shows the further advanced stage of the growth in the rod-like $SnO_2$ single crystal, and the enlarged microphotograph of the portion of [A] in Fig. 10(b) is shown in Fig. 10(c). Though the pattern of the stepped surfaces due to the elongating growth remain at the central, {101} and {011} faces develope well around it and many bunching steps are clearly recognized on these faces. That is, the thickening growth is advanced by the two dimensional layer growth from the top in succession of the elongating growth, as to expose the {101} and {011} facets of an octahedron-shape.

From these observations, it is made clear that the pyramid-type $SnO_2$ single crystal is not grown by the manner that the growth of the <110> needles precedes the thickening growth as is mentioned in the growth of the leaf-type, though their crystallization properties are same, but the pyramid-type is elongated and thickened by the two dimensional layer growth on the {101} and {011} faces toward the final stage of the growth as is shown in Fig. 4(d).

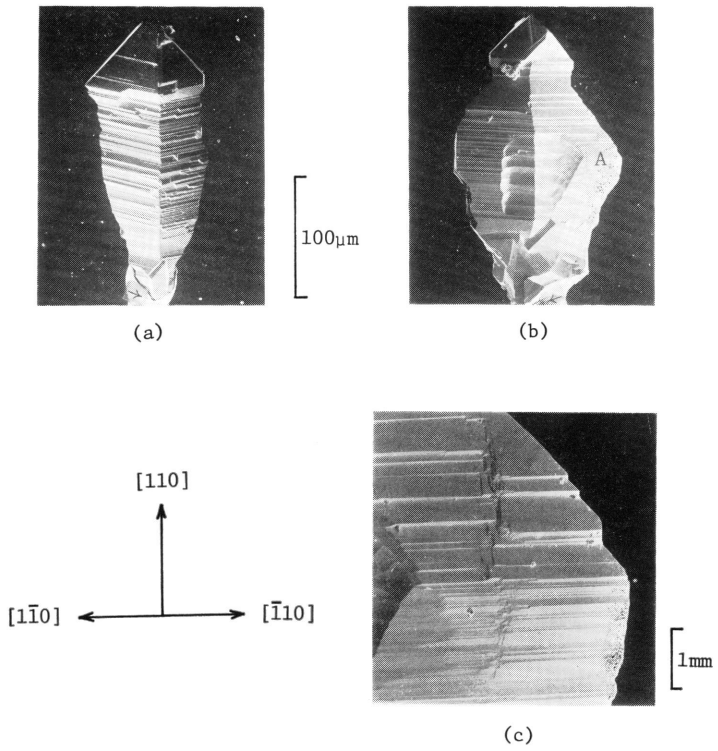


Fig. 10. Scanning electron microphotographs suggesting the growth mechanism of a pyramid-type $SnO_2$ single crystal. (a) A rod-like crystal indicating the elongating mechanism. (b) An further advancad stage of the growth; indicating the thickening mechanism. (c) The enlarged microphotopraph of the portion of [A] in (b).

5 – 3. Plate-type

Optical microphotographs of the <011> and <111> plates, which are grown by the reaction of $SnI_4$ with higher saturated wet $N_2$ gas, are shown in Figs. 11(a) and (b), respectivly. The starting point of the growth are indicated by markings ↑ in these figures. Many steps, edge-lines of which are parallel to each other, are observed on their (011) surfaces of the both-type plates and the (011) surfaces are higher at the top part than at the root due to the steps. Figures 11(c) and (d) show the enlarged microphotographs of the portion of the steps in figs. 11(a) and (b), respectiveiy. These figures show that they are bunching steps due to the two dimensional layer growth on the (011) surfaces and are piled-up from the tops to the roots in the both-type plates. The inclinations between the lines of the bunching steps and the [01$\bar{1}$] or [11$\bar{1}$] growth direction, denoted by $\alpha$ and $\beta$ in the figures, are $\alpha = 39°$ and $\beta = 79°$. These values coincide with the theoretical ones

of the angles between the $[\bar{1}1\bar{1}]$ and $[11\bar{1}]$ directions and the $[01\bar{1}]$ growth direction in the <011> plate and between the $[\bar{1}1\bar{1}]$ direction and the $[11\bar{1}]$ growth direction in the <111> plate, respectively.

From these figures, it is concluded that though the elongating growth is not clear, the thickening growth is advanced by the two dimensional layer growth from

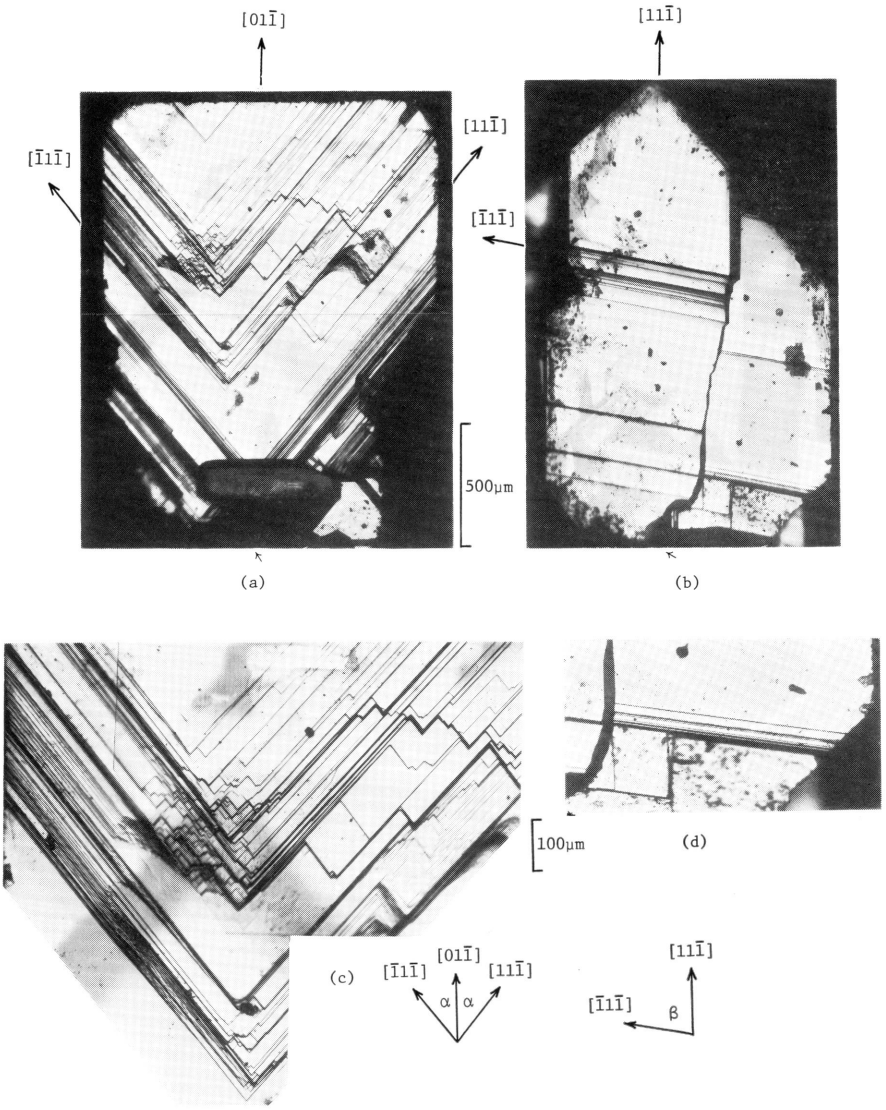


Fig. 11. Optical microphotographs of the <011> and <111> plate-type $SnO_2$ single crystals suggesting their thickening mechanism of the growth. (a) The <011> plate-type and (b) the <111> plate-type. (c) and (d) The enlarged micropotographs on the (011) surfaces of the <011> and <111> plate-types, respectively.

the top to the root in both-type plates and that the molecules taking part in the crystallizations are always associated in the <111> directions.

## 6. Summary

$SnO_2$ single crystals were grown from the vapor phase by the oxidation of $SnI_4$ at the temperature range of the growth region between 1200 ℃ and 1250 ℃ and by the hydrolysis of it between 1100 ℃ and 1150 ℃. In the oxidation, they were small and dendritic, and a great deal of powdery $SnO_2$ was prodnced. On the other hand, in the hydrolysis, they were crystallized largely and more largely in the case of the reaction with lower saturated wet $N_2$ gas. Pyramid and plate-types grew mainly in the reaction with higher saturated wet $N_2$ gas, and dendrite-types mainly in the reaction with lower one. Leaf and hollow-types were obtained in the both cases of the hydrolysis.

Though the both types of leaf and pyramid tended to crystallize into an octahedron-shape having {101} and {011} facets, their growth mechanisms were different : the leaf-type grew by the manner that the growth of <011> needles, the elongating growth, the growth mechanism of which was not clear, preceded to the thickening growth by the deposition and diffusion of molecules, and the pyramid-type elongated and thickened by the two dimensional layer growth on the {101} and {011} surfaces. The plate-types, two kinds of which were distinguished from the differences of their growth axes, thickened by the two dimensional layer growth on the (011) snrfaces, thongh their elongating growth mechanism was unknown.

The growth mechanism that the growth of needles preceded the thickening growth, which had been observed in the growth of plate-type ZnO single crystal grown by the vapor reaction of $ZnI_2$ with $H_2O$, was also observed in the growth of leaf-type.

## References

[1] J. A. Marley and T. C. MacAvoy, J. Appl. Phys. **32** (1961) 2504.
[2] T. B. Reed, J. T. Roddy and A. N. Mariano, J. Appl. Phys. **33** (1962) 1014.
[3] T. Takizawa and T. Sakurai, Japan. J. Appl. Phys. **12** (1973) 1323.
[4] B. Thiel and R. Helbig, J. Crystal Growth **32** (1976) 259.
[5] M. Hirose and Y. Furuya, Japan. J. Appl. Phys. **9** (1970) 423.
[6] M. Hirose, Japan. J. Appl. Phys. **10** (1971) 401.
[7] M. Hirose and Y. Furuya, Japan. J. Appl. Phys. **11** (1972) 423.
[8] M. Nagasawa, S. Shionoya and S. Makishima, Japan. J. Appl. Phys. **4**(1965) 195.
[9] C. G. Fonstad, A. Linz and R. H Rediker, J. Electrochem. Soc. **116** (1969) 1269.
[10] W. H. Baur, Acta Cryst. **9** (1956) 515.
[11] T. Fujiwara and S. Dohi, J. Phys. Soc. Japan **18** (1963) 1763.